Research Square

Preprints are preliminary reports that have not undergone peer review.
They should not be considered conclusive, used to inform clinical practice,
or referenced by the media as validated information.

Anti-Candida properties of 5-butyl-2-pyridine carboxylic acid, extracted from azole drug-sensitive microfungi Aspergillus fumigatus nHF-01

Vivekananda Mandal
University of Gour Banga
Rajsekhar Adhikary
University of Gour Banga
Narendra Nath Ghosh
Narendra Nath Ghosh, Pakuahat ANM High School
Sayan Poddar
Indian Institute of Technology Roorkee
VIVEKANANDA MANDAL
mandalvivek@gmail.com

University of Gour Banga

Research Article

Keywords: 5-butyl-2-pyridine carboxylic acid, Anti-Candida properties, Aspergillus fumigatus nHF-01, Candida spp., Lanosterol 14α-demethylase (CYP51) inhibitor

Posted Date: September 1st, 2026

DOI: https://doi.org/10.21203/rs.3.rs-10593573/v1

License: This work is licensed under a Creative Commons Attribution 4.0 International License.
Read Full License

Additional Declarations: No competing interests reported.

Anti-*Candida* properties of 5-butyl-2-pyridine carboxylic acid, extracted from azole drug-sensitive micro-fungi *Aspergillus fumigatus* nHF-01

Vivekananda Mandal[1], Rajsekhar Adhikary[1, 2], Narendra Nath Ghosh[3], Sayan Poddar[4] and Vivekananda Mandal[1*]

Addresses and affiliations:

[1]**Vivekananda Mandal,** Plant and Microbial Physiology and Biochemistry Laboratory, Department of Botany, University of Gour Banga, Malda, West Bengal, India; Email: mandalvivek88@gmail.com; https://orcid.org/0009-0001-3521-8144

[1]**Rajsekhar Adhikary,** Plant and Microbial Physiology and Biochemistry Laboratory, Department of Botany, University of Gour Banga, Malda, West Bengal, India; Email: radhikary468@gmail.com; https://orcid.org/0009-0005-9167-3001

[2]Department of Botany, Murshidabad Maharaja Krishnanath University, Berhampore, West Bengal, India.

[3]**Narendra Nath Ghosh,** Pakuahat ANM High School, Malda, West Bengal, India. Email: ghosh.naren13@gmail.com https://orcid.org/0000-0001-6026-4639

[4]**Sayan Poddar,** [1]Department of Bioscience and Bioengineering, Indian Institute of Technology Roorkee, Roorkee, Uttarakhand, India; Email: sayan.poddar30@gmail.com

[1*]**Vivekananda Mandal,** Plant and Microbial Physiology and Biochemistry Laboratory, Department of Botany, University of Gour Banga, Malda, West Bengal, India, Mob: +91 9679008986, Email: vivek.bot@ugb.ac.in and mandalvivek@gmail.com; **ORCID:** https://orcid.org/0000-0001-6523-8069

[*]**Correspondence:** Professor Vivekananda Mandal, Plant and Microbial Physiology and Biochemistry Laboratory, Department of Botany, University of Gour Banga, Malda, West Bengal, India, Mob: +91 9679008986, Email: vivek.bot@ugb.ac.in and mandalvivek@gmail.com; **ORCID:** https://orcid.org/0000-0001-6523-8069

Running Title: Anti-*Candida* potentials of 5-butyl-2-pyridine carboxylic acid

Highlights

- 5-butyl-2-pyridinecarboxylic acid is produced by *Aspergillus fumigatus* nHF-01
- It showed potent anti-*Candida* activity.
- The MIC and MFC values ranged from 0.129 ± 0.013 to 0.258 ± 0.012 mg/ml.
- It has a time-kill endpoint within 15 hours.
- It has FIC indices with clotrimazole and luliconazole.
- It has moderate biofilm inhibition and destabilization efficacy.
- It acts on the ergosterol biosynthetic enzyme Lanosterol 14α-demethylase (CYP51).

Abstract

Objectives: This study aimed to evaluate the effects of 5-butyl-2-pyridinecarboxylic acid, a potent antimicrobial compound from *Aspergillus fumigatus*, on growth inhibition, biofilm formation, biofilm destabilization, and cellular integrity in four *Candida* species.

Materials and Methods: The anti-*Candida* activity of 5-butyl-2-pyridinecarboxylic acid was assessed using disk diffusion and microdilution assays to determine minimum inhibitory concentration (MIC) and minimum fungicidal concentration (MFC). Growth kinetics were monitored through growth curve and time-kill assays, while synergistic effects with standard antifungal drugs were evaluated using fractional inhibitory concentration (FIC) indices. Cellular damage was analyzed by scanning electron microscopy (SEM) and lactate dehydrogenase (LDH) release assays. Biofilm inhibition and destabilization were determined using microtiter plate assays with crystal violet staining. A molecular docking study was done to predict the potential target of action.

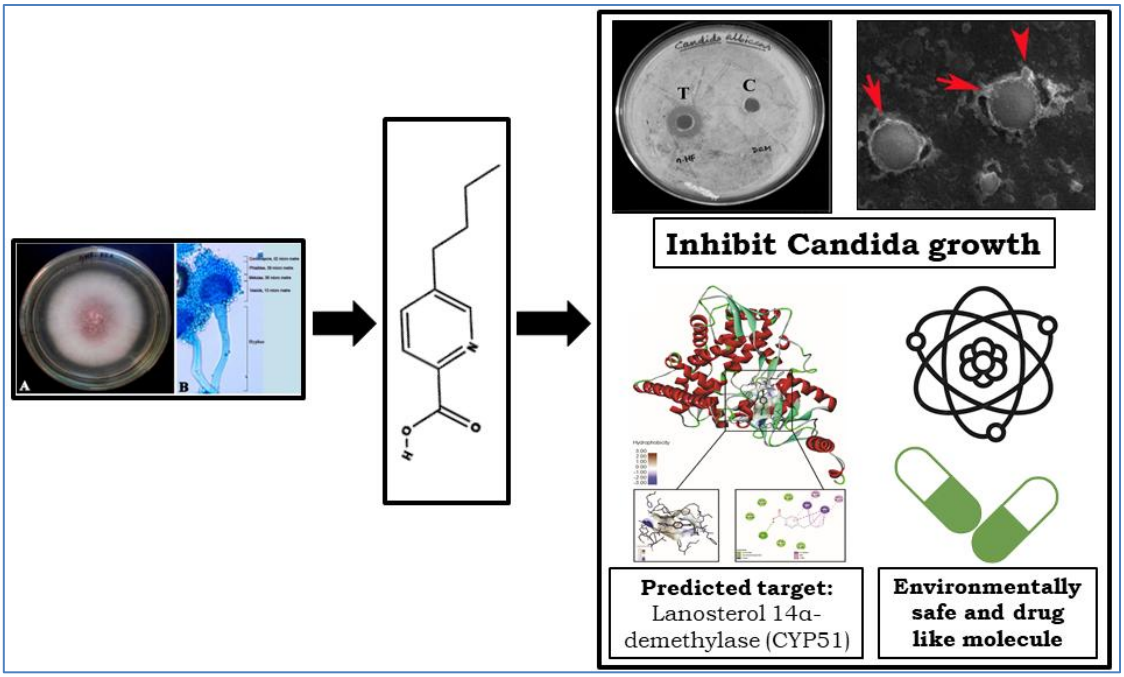
Results: The compound exhibited potent inhibitory activity, with MIC and MFC values ranging from 0.129 ± 0.013 to 0.258 ± 0.012 mg/ml. At concentrations between 0.128 and 0.258 mg/mL, it induced rapid loss of viability and complete lethality within 15 hours. SEM and LDH assays revealed significant cell wall disruption and increased permeability. Time-kill kinetics confirmed potent fungicidal activity. The compound also showed synergistic effects with clotrimazole and luliconazole against *C. albicans* and *C. glabrata*, while an additive effect was observed against *C. parapsilosis*. It showed antibiofilm activity as compared to usnic acid. 5-butyl-2-pyridine

carboxylic acid was predicted to be a potential target of the ergosterol biosynthetic enzyme Lanosterol 14α-demethylase (LDM) (CYP51) of *C. glabrata* and its correlated isoform ERG11 of *C. albicans*.

Conclusions: This study highlights the promising anti-*Candida* potential of 5-butyl-2-pyridine carboxylic acid. By disrupting cell walls, increasing membrane permeability, exhibiting synergism with conventional antifungals, and being predicted to inhibit 14α-demethylase (CYP51), the compound represents a potential lead candidate. Further safety and mechanistic studies are needed to explore its application in antifungal drug development.

Keywords: 5-butyl-2-pyridine carboxylic acid; Anti-*Candida* properties; *Aspergillus fumigatus* nHF-01; *Candida* spp.; Lanosterol 14α-demethylase (CYP51) inhibitor.

Graphical abstract



Introduction

Candida species represent a biologically diverse group of fungi belonging to the family Saccharomycetaceae, displaying both ascomycetous and basidiomycetous affinities. Currently, approximately 200 species are recognized within the genus (Silva et al., 2012). Members of *Candida* spp. are widely distributed in nature and are frequently found on humans as commensals. However, under favorable conditions, such as immune suppression, they can transform into opportunistic pathogens capable of causing superficial and systemic

infections (Haynes, 2001; Sanglard & Odds, 2002). The gastrointestinal tract, along with mucosal epithelial tissues, is considered the major habitat for commensal *Candida* species (Mishra and Koh, 2021). Clinical manifestations include infections of the oral cavity, esophagus, gastrointestinal tract, vagina, endocardium, nervous system, bone, and joints (Sobel, 2007). Among the numerous species, *Candida albicans* is the most notorious, being associated with nearly 40% of cerebral mycoses (Riera et al., 2022) and responsible for life-threatening systemic infections in immunocompromised or severely debilitated individuals (Pfuller et al., 2011). At least 30 *Candida* species have been reported to have clinical importance (Silva et al., 2012), though *Candida albicans*, *C. glabrata*, *C. tropicalis*, *C. parapsilosis, C. krusei,* and *C. guilliermondii* remain the most frequently isolated from clinical cases (Bilal et al., 2023; Cabrera-Guerrero et al., 2025). Importantly, *C. albicans* alone is estimated to account for 45-50% of candidiasis cases worldwide (Del Palacio et al., 2009). Over the past few decades, the incidence of candidiasis has increased significantly, making it a major public health concern (Pfuller et al., 2011). Candidiasis encompasses a spectrum of diseases, from relatively mild mucosal infections to invasive systemic mycoses with high morbidity and mortality. Candidemia, the bloodstream infection caused by *Candida* species, has emerged as one of the most alarming nosocomial fungal infections worldwide, especially among hospitalized and immunocompromised patients (Sobel, 2007). The ability of *Candida* spp. to form robust biofilms on both biotic and abiotic surfaces, including medical devices such as catheters and prosthetics, amplifies this problem (Soliman, 2017). Biofilms provide an effective protective matrix of extracellular polymeric substances, rendering *Candida* communities resistant to host immune responses and antifungal therapies (Sharma, 2019). Consequently, biofilm-associated infections are notoriously difficult to eradicate and are a leading cause of mortality in patients undergoing surgical interventions and prolonged hospitalization (Oluwole, 2022). This biofilm-forming capacity underscores *Candida*'s status as one of the most formidable fungal pathogens in clinical medicine.

The treatment of *Candida* infections remains a significant clinical challenge due to the rise of antifungal resistance and limited therapeutic options. Currently, the primary classes of anti-*Candida* drugs include azoles (e.g., fluconazole), polyenes (e.g., amphotericin B), echinocandins (e.g., caspofungin), and pyrimidine analogs (e.g., flucytosine). The growing incidence of multidrug-resistant *Candida* infections has also posed a serious therapeutic challenge, urging the pharmaceutical sector to identify new antifungal strategies. Although azole derivatives such as voriconazole and posaconazole have broadened the therapeutic arsenal against candidiasis (Arendrup, 2013), the emergence of drug resistance continues to limit their effectiveness. Infections caused by *Candida* not only represent a significant healthcare burden but also contribute to substantial global mortality rates. Furthermore,

candidiasis is not limited to humans; it affects a wide range of vertebrates, underscoring its broad pathogenic potential. As such, the study of *Candida* biology, its commensal-to-pathogen transition, and its resistance mechanisms remains crucial in order to develop effective therapeutic strategies. The duality of *Candida* species as commensals and opportunistic pathogens exemplifies their evolutionary adaptability and underscores the necessity for ongoing research into antifungal drug development, prevention, and management. Emerging therapeutic strategies include novel azole derivatives, combination therapies, and natural product-based antifungals, which are being investigated to overcome resistance and enhance treatment efficacy (McCarty & Pappas, 2016; Arendrup & Patterson, 2017; Perfect, 2017).

Although numerous microbial metabolites have been investigated for antifungal activity, low-molecular-weight heteroaromatic compounds, including carboxylic acid derivatives, remain insufficiently studied against *Candida* species (Perfect, 2017; Arendrup & Patterson, 2017). In a previous study, 5-butyl-2-pyridine carboxylic acid was isolated and structurally characterized from *Aspergillus fumigatus* nHF-01 and showed broad-spectrum antibacterial activity, with MIC and MBC values ranging from 0.069 ± 0.0034 to 1.12 ± 0.052 mg/mL and from 8.925 ± 0.39 to 17.85 ± 0.78 mg/mL, respectively. In contrast, the MBC ranged from 8.925 ± 0.40 to 17.85 ± 0.776 mg/mL and from 0.069 ± 0.0034 to 0.139 ± 0.0065 mg/mL against human pathogenic Gram-positive and Gram-negative bacteria, respectively (Mandal et al., 2022), but its antifungal potential was not examined. The present study was therefore undertaken to evaluate this compound based on its distinct pyridine scaffold, favorable physicochemical properties, and preliminary antimicrobial indications, which are considered desirable features in antifungal lead discovery (McCarty & Pappas, 2016; Perfect, 2017). The aim of the present study was to evaluate the antifungal potency, antibiofilm efficacy, combinatorial relationship with conventional antifungal drugs, and in silico prediction of the mode of action of 5-butyl-2-pyridine carboxylic acid from *Aspergillus fumigatus* nHF-01. To the best of our knowledge, this is the first report describing the anti-*Candida* activity of 5-butyl-2-pyridine carboxylic acid, including its fungicidal kinetics, antibiofilm effects, combinatorial interactions with clinically used azoles, and predicted molecular targets. Collectively, these findings address an existing knowledge gap and provide a foundation for further investigation of this fungal metabolite as a potential antifungal lead.

Material and Methods

1. Strains, Culture Conditions, and Extraction of 5-Butyl-2-Pyridine Carboxylic Acid

The microfungus *Aspergillus fumigatus* nHF-01 (GenBank Acc. No. MN190286) was cultured and maintained on Potato Dextrose Agar (PDA) at 28 °C, with subculturing performed at 5–7 day intervals to ensure active growth and viability (Mandal et al., 2022). The production and purification of 5-butyl-2-pyridinecarboxylic acid were performed following the protocol described by Mandal et al. (2022). Briefly, *A. fumigatus* nHF-01 was cultured in submerged malt extract broth (MEB) and yeast extract (YE) broth at 20 °C for 10 days in a shake flask at 100 rpm, and the culture was centrifuged to obtain the cell-free culture aliquot. The active fraction was extracted with dichloromethane (DCM) and concentrated under reduced pressure using a rotary evaporator. The pure fraction was collected by a preparative multidimensional RP-HPLC system (Waters Alliance, 2695, MDLC, UV–Vis detector 2487) equipped with a C_{18} column, with an elution solvent system of 0.5% H_3PO_4, 90% acetonitrile, and 0.1% trifluoroacetic acid as mobile phase with a flow rate of 1.0 mL/min at 30 ± 2 °C and detected at 246 nm. The fractions were collected and tested for potential anti-*Candida* activity (Mandal et al., 2022).

2. Anti-*Candida* Assay of 5-butyl-2-pyridine Carboxylic Acid

To evaluate the anti-*Candida* activity of the bioactive compound 5-butyl-2-pyridine carboxylic acid, four pathogenic *Candida* strains were selected: *C. albicans* MTCC 183, *C. glabrata* MCC 1445, *C. parapsilosis* MCC 1438, and *C. tropicalis* MCC 1434. The strains were obtained from MTCC (Chandigarh, India) and MCC (Pune, India), and routinely maintained on Sabouraud Dextrose Agar (SDA; 4% dextrose, 1% mycological peptone, and 1.5% agar, w/v; pH 5.6) at 37 °C. The compound (5.0 mg/mL) was tested by the agar well diffusion method, with clotrimazole (0.25 mg/mL) and luliconazole (0.25 mg/mL) as positive controls, and dichloromethane (DCM) as a negative control (Mandal et al., 2022).

3. Determination of MIC and MFC

The minimum inhibitory concentration (MIC) was determined using the microdilution method, and the minimum fungicidal concentration (MFC) was evaluated by the spread plate method (Nový et al., 2015; Mandal et al., 2022; Adhikary et al., 2025). Tests were performed in 96-well microtiter plates, and absorbance was measured at 630 nm in a microplate reader (Bio-Rad iMark™, USA). MICs were defined as the lowest concentration of the compound at which no visible growth was observed (Espinel-Ingroff et al., 2002). The yeasts strains were grown overnight in Sabouraud Dextrose broth (SDB) medium at 37 °C diluted with fresh SDB medium to maintain the final concentration according to the McFarland standard (0.5 at 620 nm, ~ 1.5×10^8 CFU/mL and treated with 5-butyl-2-pyridine carboxylic acid in the final concentration range from 0.517 to 0.004 mg/ml (using DCM) and incubated at 24 hrs at 37 °C and the optical density was recorded at 600 nm using a microplate reader (*i*Mark,

Bio-Rad, USA). Clotrimazole (0.031 to 10 mg/mL) served as the reference antifungal drug. For MFC determination, concentrations higher than the MIC were plated on SDA and incubated at 37 °C for 48 hrs. The concentration at which no visible colonies developed was recorded as the MFC (Espinel-Ingroff et al., 2002). Negative controls contained solvent only, while clotrimazole served as the positive control. All experiments were performed in triplicate.

4. Effect on Growth and Viability of *Candida* Strains

The effect of the compound on the growth and viability of the four *Candida* strains was evaluated as described by Mandal et al. (2022). Briefly, exponentially growing 12 hrs cells, diluted to McFarland standard (0.5 at 620 nm, ~ 1.5×10^8 CFU/mL) with sterile fresh SDB broth, were inoculated (10 µL) to 230 µL of sterile fresh SDB broth, and treated with 10 µL of the purified compound to achieve a final concentration of 2×MIC for the respective pathogens and incubated at 37 °C for 30 hrs. Cell growth was monitored at 15 min, 30 min, 1 hr, and 3 hr intervals by measuring the optical density of the microplates at 600 nm using a microplate reader (*i*Mark, Bio-Rad, USA). Simultaneously, 10 µL cultures were removed, diluted in serial decimal dilutions (10^{-2}-10^{-8}), spread onto SDA plates, and incubated at 37 °C for 48 hrs to measure colony-forming units (CFU) and report CFU/mL as log CFU/mL. For comparison, the effects of clotrimazole and luliconazole (conc. 2xMIC) were also evaluated against the same *Candida* strains.

5. Determination of Time-Kill Endpoints

Time-kill studies were performed at the MFC of the compound (0.258 mg/mL against *C. albicans* and *C. tropicalis*, whereas 0.517 mg/mL against *C. glabrata* and *C. parapsilosis*), as described by Mandal et al. (2022). The compound was applied to log-phase cultures (OD_{620} = 0.5, McFarland standard) of *Candida* strains in SDB medium, incubated at 37 °C, and 10 µL of culture was sampled at 30 min and 3 hrs intervals for 30 hrs, then spread on SDA plates and incubated at 37 °C for 48 hrs. Viable counts were determined as log CFU/mL, and kill curves were plotted against incubation time. Fungicidal efficacy was defined as a reduction of ≥3 log CFU/mL relative to the initial inoculum (McGinnis and Rinaldi, 1996; Espinel-Ingroff et al., 2002; Hall et al., 2017).

6. Effect on Cellular Integrity and Morphology

To assess cellular damage, actively growing *Candida* cells in SDB medium at 37 °C were treated with the compound at 2×MIC. Lactate dehydrogenase (LDH) release was measured from cell-free lysates after 30, 60, and 480 min of incubation. Briefly, 10 µL of the compound was added to 90 µL of 12 hrs-old cultures to achieve a final concentration twice the MIC (2×MIC) of the pathogen, and the cultures were incubated at 37 °C for up to 8 hrs. Parallel cultures were sonicated (Probe Sonicator PKS-250FM, USA; 95% power, 2s pulse, 20 °C, 10 strokes) to obtain total LDH release. Untreated cultures served as negative controls.

For morphological analysis, treated cells were washed with sterile PBS (100 mmol/L, pH 7.0), fixed, and processed for scanning electron microscopy (SEM) using a Zeiss EVO 18 microscope with a Quorum Q150R ES sputter coater (Mandal et al., 2022).

7. Antibiofilm and Biofilm Destabilization Assays

Antibiofilm assays were performed in 96-well plates seeded with *Candida* suspensions (OD_{610} = 0.6, ~1 × 10^6 cells/mL). The compound was tested at ⅛ MIC, ¼ MIC, ½ MIC, and MIC concentrations (0.016-0.129 mg/mL, w/v). Usnic acid served as a positive control, while untreated cultures were negative controls (Mandal et al., 2022). After 24 h at 37 °C, biofilm biomass was quantified by crystal violet (CV) staining at OD_{595} nm. Biofilm inhibition was calculated as:

$$\% \text{ Biofilm inhibition} = 100 \times \{(OD_{595\ control} - OD_{595\ test}) / OD_{595\ control}\}$$

For biofilm destabilization, 18 h preformed biofilms were treated with ¼ MIC, ½ MIC, and MIC of the compound for 24–36 hrs, followed by CV staining to measure residual biofilm biomass.

8. Combinatorial Effect with Anticandidal Drugs

Drug-compound interactions were analyzed using the checkerboard microdilution method (Marchetti et al., 2000; Mandal et al., 2022). Actively grown *Candida* cultures (4-5×10^6 CFU/mL) were maintained in Sabouraud Dextrose Broth (SDB) at 37 °C for 14 hrs. AMC and the drugs (10 µL each) at their final MIC values were added to 180 µL of sterile SDB medium, and 10 µL of appropriately diluted active culture was inoculated in 96-well plates and incubated at 37 °C for 24 hrs using a microplate reader (*i*Mark, Bio-Rad, USA). Growth was measured at OD_{620} nm. The fractional inhibitory concentration index (FICI) was calculated according to Fatsis-

Kavalopoulos et al. (2024) and Adhikary et al. (2025). Interactions were classified as synergy (FICI < 0.5), additive (0.5 ≤ FICI = 1), indifference (1 < FICI < 4), or antagonism (FICI ≥ 4) (Fatsis-Kavalopoulos et al., 2024).

The fractional inhibitory concentration index (FICi) is calculated using the formula as follows.

$$FICi = \frac{C_A}{MIC_A} + \frac{C_B}{MIC_B}$$

where MIC_A and MIC_B are the minimum inhibitory concentrations of MIC_A and MIC_B, and C_A and C_B are the concentrations inhibiting *Candida* spp. growth in combination.

9. Molecular interactions and Molecular Dynamics (MD) Simulations

Molecular docking studies were performed to predict the binding interactions of 5-butyl-2-pyridine carboxylic acid with target proteins from *Candida* spp., retrieved from the Protein Data Bank (https://www.rcsb.org; Table S2). Docking was carried out using AutoDock Vina after protein preparation (removal of heteroatoms, addition of polar hydrogens, and charge assignment). Docking scores were analyzed with Discovery Studio (Bheemarasetti et al., 2018). Clotrimazole, flucytosine, and voriconazole were used as reference antifungal ligands.

MD simulations were performed using GROMACS v2023.3 with the CHARMM36 all-atom force field and the modified TIP3P water model, as implemented in GROMACS. Ligand parameters were generated using the SwissParam (2022) web server. Each docked receptor-ligand complex was placed in a dodecahedral simulation box, ensuring a minimum distance of 12 Å from the complex to the box boundaries, and solvated with explicit water molecules. To achieve system neutrality and physiological conditions, sodium (Na^+) and chloride (Cl^-) ions were added to a final salt concentration of 0.15 M. Subsequently, energy minimization was performed using the steepest descent algorithm for 5000 steps until the maximum force converged below 1000 kJ/mol nm^{-1}. The systems were then equilibrated in two stages. First, position restraints were applied to the receptor-ligand complexes, followed by a 100 ps NVT equilibration using a leapfrog integrator with a 2 fs time step, LINCS constraints, and temperature coupling at 300 K using V-rescale modified Berendsen thermostat. This was followed by a 100 ps NPT equilibration for 100 ps with a 2 fs time step, maintaining pressure at 1 bar using the C-rescale barostat and temperature at 300 K. After equilibration, each system was subjected to a 100 ns production MD simulation using a leapfrog integrator with a 2 fs time step. Trajectory analyses focused on key dynamic properties, including root-mean-square deviation (RMSD), root-mean-square fluctuation (RMSF), radius of gyration (Rg), and protein-ligand distance. RMSD, RMSF, and Rog were calculated using standard GROMACS tools (gmx rms,

gmx rmsf, and gmx gyrate), while the distance between the centre of mass of the protein and ligand was computed using the gmx distance tool.

10. In-silico Toxicity Prediction Assay

In silico toxicity was assessed using ProTox-III (https://tox.charite.de/protox3) (Banerjee et al., 2024), while environmental toxicity was predicted using admetSAR (http://lmmd.ecust.edu.cn/admetsar1/predict/) (Cheng et al., 2012). Drug-likeness was evaluated by Lipinski's Rule of Five through the SCFBio-IITD server (http://www.scfbio-iitd.res.in/software/drugdesign/lipinski.jsp) (Jayaram et al., 2012).

11. Statistical analysis

All experiments and their corresponding treatments were performed in triplicate. Data are presented as mean ± standard deviation (SD).

Results

1. Anti-Candida activity and determination of MIC and MFC of 5-butyl-2-pyridinecarboxylic acid

The bioactive compound 5-butyl-2-pyridinecarboxylic acid exhibited potent growth inhibitory effects against all tested *Candida* species, producing inhibition zones of 15-20 mm at a concentration of 5.0 mg/ml (Figure S1). The MIC and MFC values of the compound ranged from 0.064 to 0.129 mg/mL and from 0.258 to 0.517 mg/mL, respectively (Table 1). Among the tested species, *C. tropicalis* displayed the lowest MIC value (0.064 mg/ml), while the remaining strains had MICs of 0.129 mg/ml. The lowest MFCs (0.258 mg/ml) were observed in *C. albicans* and *C. tropicalis*, whereas *C. glabrata* and *C. parapsilosis* exhibited the highest MFC values (0.517 mg/ml). In comparison, standard antifungal drugs, including clotrimazole, luliconazole, terbinafine, and usnic acid, showed distinct MIC and MFC values (Table 1).

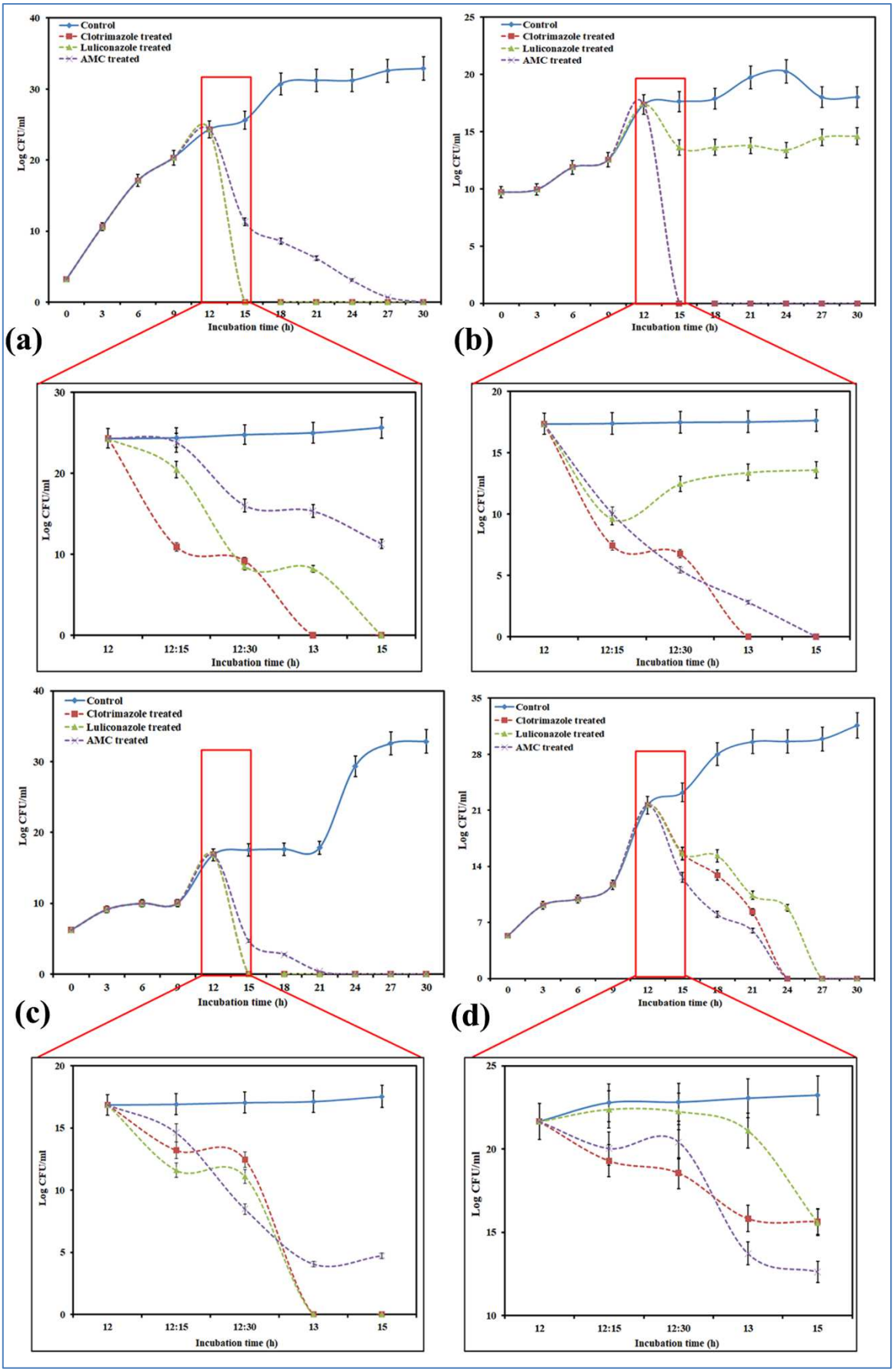
Table 1: MIC and MFC values of 5-butyl-2-pyridine carboxylic acid against *Candida* strains.

Sl. No.	Organisms	MIC values (mg/ml)					MFC values (mg/ml)			
		AMC	AFD				AMC	AFD		
			CLT	LLC	TRB	UA		CLT	LLC	TRB
1	*C. albicans*	0.129± 0.001	0.125± 0.01	0.125±0.001	05±0.023	0.16±0.08	0.258±0.012	0.25±0.13	0.25±0.1	10±0.07
2	*C. glabrata*	0.129± 0.09	0.25±0.08	0.25±0.78	2.5±0.6	0.08±0.004	0.517±0.07	0.5±0.026	0.5±0.003	05±0.032
4	*C. parapsilosis*	0.129± 0.067	0.25±0.08	0.5±0.25	0.5±0.023	0.08±0.004	0.517±0.26	0.5±0.026	01±0.001	01±0.001
3	*C. tropicalis*	0.064± 0.11±	0.125±0.11	0.5±0.12	2.5±0.13	0.04±0.002	0.258±0.18	0.25±0.06	01±0.001	05±0.025

Here, the abbreviations stand for **AMC**- 5-butyl-2-pyridine carboxylic acid; **AFD**- Antifungal drug (**CLT**- Clotrimazole; **LLC**- Luliconazole; **TRB**- Terbinafine and **UA**- Usnic acid). Here, the values are the average of triplicate trials ± SE.

2. Effect on Growth and Viability of *Candida* Strains

Application of 5-butyl-2-pyridine carboxylic acid (MIC×2) led to a sharp decline in the viability of 12 hr-old cells across all strains within 30 minutes of treatment (Figure 1a-d). Notably, *C. glabrata* reached zero CFU within 3 h of treatment (at 15 hr) with the compound (Figure 1b), while *C. albicans*, *C. tropicalis*, and *C. parapsilosis* required 9-15 h to achieve complete loss of viability after the treatment (Figure 1a, c, and d). Unlike the test compound, standard antifungal drugs (clotrimazole and luliconazole) at their respective double MICs (MIC×2) caused rapid loss of viability within 60 min across all strains. Interestingly, *C. glabrata* regained partial viability after 30 min of luliconazole treatment, a phenomenon not observed with 5-butyl-2-pyridinecarboxylic acid.


(a)
(b)
(c)
(d)
Control
Clotrimazole treated
Luliconazole treated
AMC treated
Log CFU/ml
Incubation time (h)
12
12:15
12:30
13
15

1

Fig. 1: Effect of the AMCs on the growth and viability of *Candida* strains. The figure indicates the treatment against (**a**) *C. albicans*, (b) *C. glabrata*, (c) *C. parapsilosis*, and (**d**) *C. tropicalis.* Herein, the blue, red, green, and violet lines indicate the untreated control set, the clotrimazole-treated, the luliconazole-treated, and the 5-butyl-2-pyridine carboxylic acid-treated, respectively, at MIC×2 concentrations. The marked regions are enlarged to observe the growth-inhibition pattern after the immediate application of AMC and standard drugs.

3. Time-Kill Endpoints

The time-kill kinetics assay confirmed the fungicidal nature of the compound. *C. glabrata* and *C. parapsilosis* exhibited complete killing within 12-13 hrs, whereas *C. albicans* and *C. tropicalis* required 15-16 hrs. There was an abrupt reduction in *C. glabrata* viability from 17.36 to 5.46 Log CFU/ml within just 30 min of treatment (Figure 2a). Collectively, these results highlight the compound's intense and rapid fungicidal action.

4. Effect on Cellular Integrity and Morphology

Lactate dehydrogenase (LDH) leakage assays revealed a progressive increase in LDH activity in *C. glabrata* treated with the compound, correlating with a reduction in CFU/ml over 480 min of incubation (Figure 2b). Positive controls (sonicated cells) showed maximal LDH release, but only a moderate decline in CFU. The other *Candida* species exhibited reduced viability without significant LDH leakage. The SEM studies showed that the anticandidal compound 5-butyl-2-pyridine carboxylic acid formed pores in the cells, leading to distortion of cellular morphology in *C. albicans* and *C. glabrata* (Figure 2c-f). These results align with LDH assay and SEM studies from earlier studies, which show that *Candida* cells exposed to antifungal metabolites exhibit surface blebbing, ruptured morphology, and pore formation (Mandal et al., 2022).

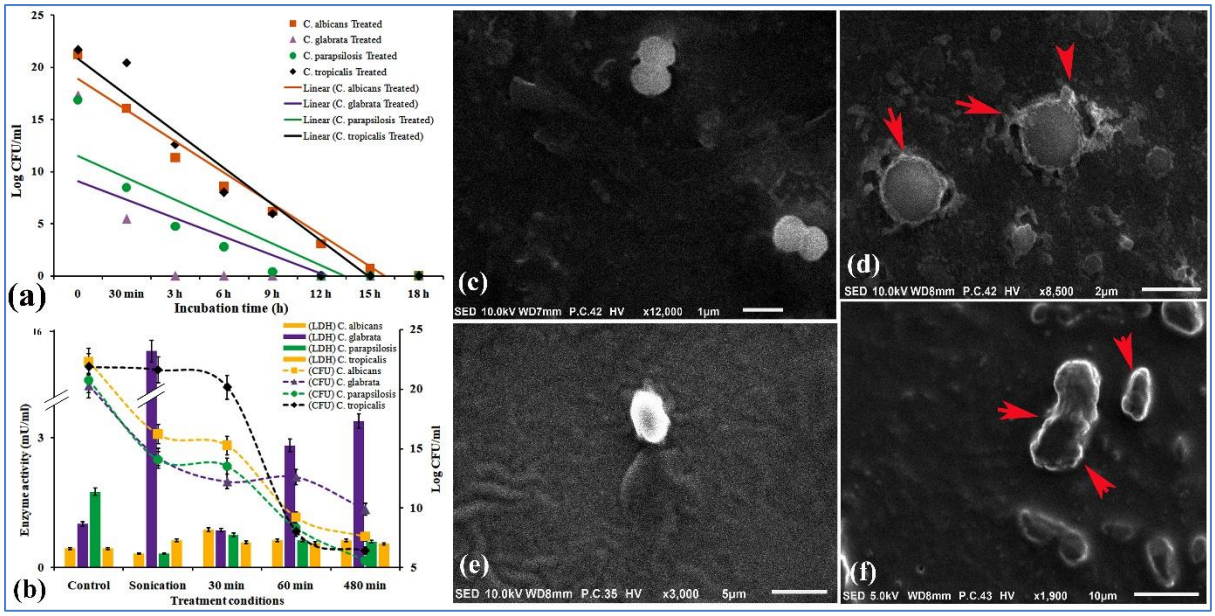


Fig. 2: Mode of action of 5-butyl-2-pyridine carboxylic acid. (a) Time-kill kinetics; **(b)** Effect of AMC on cellular integrity. In the figure, LDH is shown as bars, and the respective CFU are shown as dotted lines. Here, the bar and line color indicates yellow for *C. albicans,* violet for *C. glabrata,* green for *C. parapsilosis,* and black for *C. tropicalis*; and **(c-f)** SEM photomicrographs of *C. albicans* and *C. glabrata* cells treated with 5-butyl-2-pyridine carboxylic acid. Here (**c** and **e**) are the untreated control cells of *C. albicans* and *C. glabrata* (magnification: ×12000, ×3000, respectively); (**d**) treated *C. albicans* cells (magnification: ×8500) after 3 hrs incubation; (**f**) treated *C. glabrata* cells (magnification: ×1900) after 3 hrs incubation. The significant morphological changes have been marked with red arrows.

5. Antibiofilm and Biofilm Destabilization Assays

The compound demonstrated antibiofilm activity against all *Candida* spp., except *C. tropicalis*, compared with usnic acid (Table S1; Figure 3a). Compared with the untreated control cells, the treatment at MIC values resulted in biofilm inhibition rates of 69.34% (*C. albicans*), 67.91% (*C. glabrata*), 71.11% (*C. parapsilosis*), and 18.57% (*C. tropicalis*). However, at MIC/2 and MIC/4, biofilm formation has gradually increased. The compound also destabilized 18-hr-preformed (18 h) biofilms of *C. albicans* (16%), *C. glabrata* (19%), *C. parapsilosis* (9%), and *C. tropicalis* (9%) at their respective MIC doses (Figure 3b). These results align with previous studies showing antifungal metabolites with moderate biofilm inhibition (Ruan et al., 2021; Mandal et al., 2022).

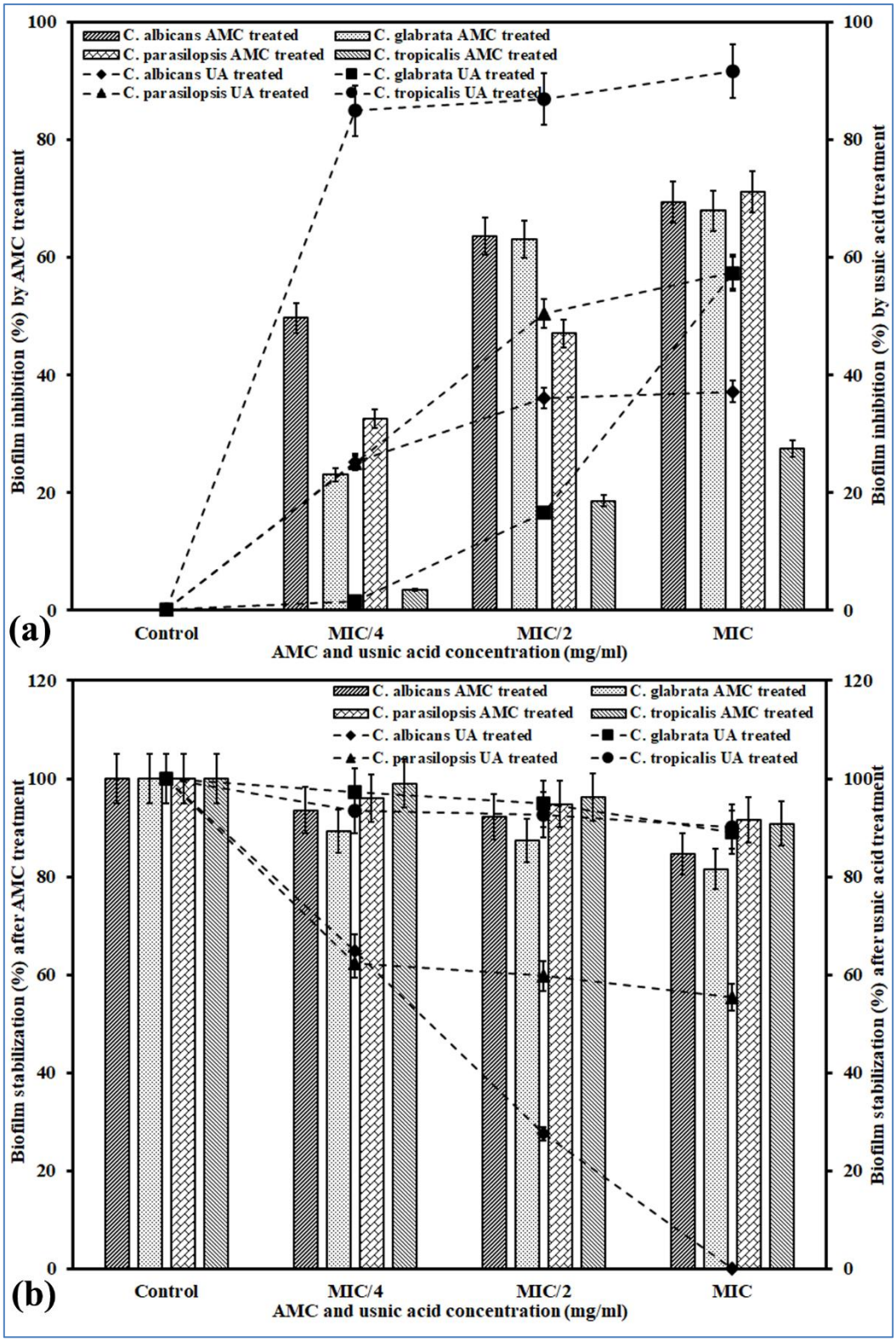


Fig. 3: Effect of 5-butyl-2-pyridine carboxylic acid on **(a)** *Candida* biofilm formation inhibition and **(b)** destabilization of preformed biofilm. Here, the bar indicates AMC (5-butyl-2-pyridine carboxylic acid) treatment, and the dotted line indicates Usnic acid (UA) treatment. Here, the bars indicate AMC treatment, and the lines indicate usnic acid treatment.

6. Combinatorial Effect with Anticandidal Drugs

Checkerboard assays revealed synergistic and partial synergistic interactions between 5-butyl-2-pyridinecarboxylic acid and conventional antifungal drugs (clotrimazole, luliconazole). The compound synergized with luliconazole against *C. albicans* and with clotrimazole against *C. glabrata*, while an additive effect was observed against *C. parapsilosis*. For *C. tropicalis*, both synergistic and additive effects were noted (Table 2). Such interactions are consistent with reports showing that combinations of antifungal agents enhance efficacy by targeting distinct cellular processes (Cheesman et al., 2017; Gao et al., 2022).

Table 2: FIC index with 5-butyl-2-pyridine carboxylic acid, Luliconazole, and Clotrimazole against *Candida* spp.

Organisms	Antifungal agents	FIC index	Inference
C. albicans	Luliconazole	0.25	Synergistic
	Clotrimazole	0.375	
C. glabrata	Luliconazole	0.375	
	Clotrimazole	0.375	
C. parapsilosis	Luliconazole	0.625	Additive
	Clotrimazole	0.75	
C. tropicalis	Luliconazole	0.25	Synergistic
	Clotrimazole	0.625	Additive

7. Molecular Interactions and Molecular Dynamics Simulation with CYP51

Molecular interaction studies demonstrated that 5-butyl-2-pyridinecarboxylic acid interacted with multiple yeast proteins, including cholesterol esterase (1llf, -6.5 kcal/mol), lanosterol 14α-demethylase (5jlc, 5v5z, Q9UR36 -6.6, -6.5, -6.2 kcal/mol, respectively), sterol-binding StART domain (6bym, -6.1 kcal/mol), β-glucan synthase (8jzn, -6.3 kcal/mol), N-myristoyl transferase (1nmt, -6.2 kcal/mol), and serine/threonine protein phosphatase (5jpe, -6.4 kcal/mol) (Table S2). Unlike voriconazole and clotrimazole, which lacked hydrogen bonding in some interactions, the compound consistently formed hydrogen bonds (<4.0 Å) along with hydrophobic π-bonds, suggesting stronger and more stable binding (Table S3, Figure 4).

The anti-*Candida* compound 5-butyl-2-pyridine carboxylic acid exhibited the strongest binding affinity toward lanosterol 14α-demethylase (CYP51) from *C. glabrata* (PDB ID: 5JLC), with an XP Glide score of –6.6 kcal/mol

(Figure 5a). A 100 ns molecular dynamics (MD) simulation was performed to evaluate the stability of the protein–ligand complex. The protein backbone RMSD increased during the initial equilibration phase (0–15 ns), reaching ~0.45–0.50 nm, followed by stable fluctuations for the remainder of the simulation, indicating structural equilibration and maintenance of a stable global fold (Figure 5b). The ligand RMSD showed a comparable trend with slightly higher fluctuations but remained stable throughout, suggesting a consistent binding orientation within the active site (Figure 5c). The radius of gyration (Rog) decreased during the early phase of the simulation and stabilized around ~2.55 nm, indicating modest protein compaction followed by sustained structural stability (Figure 5d). Residue-wise RMSF analysis revealed higher flexibility at the N- and C-termini, while most internal residues exhibited low fluctuations (<0.2 nm), reflecting a rigid protein core with localized flexibility in loop regions (Figure 5e). The center-of-mass distance between the protein and ligand remained stable at ~1.4–1.6 nm throughout the simulation, with only transient deviations and no evidence of ligand dissociation, confirming the stability of the protein–ligand complex over the 100 ns timescale (Figure 5f).

8. Toxicity Prediction and Drug-Likeness

The probable toxicity of 5-butyl-2-pyridine carboxylic acid was evaluated using in silico approaches to ensure its safe therapeutic application and environmental disposal (Table S4). Predictions indicated that the compound is non-carcinogenic, non-mutagenic, non-cytotoxic, and non-immunotoxic, although it exhibited hepatotoxic potential. The probability of its overall non-toxicity was estimated to exceed 70%. Further analysis using ProTox-III and ADMETSAR classified the compound as toxicity class 3, with an estimated oral LD_{50} of 180 mg/kg and 2.5409 mol/kg body weight for acute toxicity in rats. ADME-Tox predictions revealed favorable pharmacokinetic properties. The compound demonstrated high probabilities for blood–brain barrier penetration (0.9547), intestinal absorption (0.9951), and Caco-2 cell permeability (0.7789). It was further predicted to be a non-inhibitor of both P-glycoprotein (0.9881) and renal organic cation transporter (0.8904), with subcellular localization at the plasma membrane (0.4770). Weak inhibition of hERG (0.9546) was noted, but the compound was predicted to be non-toxic in the Ames mutagenicity test (0.973) and readily biodegradable in the environment (0.8747) (Table S4). Drug-likeness evaluation based on Lipinski's Rule of Five confirmed the compound's suitability as a drug candidate, with a molecular mass of 179 Da (<500 Da), one hydrogen bond donor, three hydrogen bond acceptors, a logP value of 2.1224, and a molar refractivity of 49.808. Collectively, these findings suggest that 5-butyl-2-pyridine carboxylic acid has a favorable pharmacological and environmental safety profile, supporting its potential as a promising antifungal lead compound.

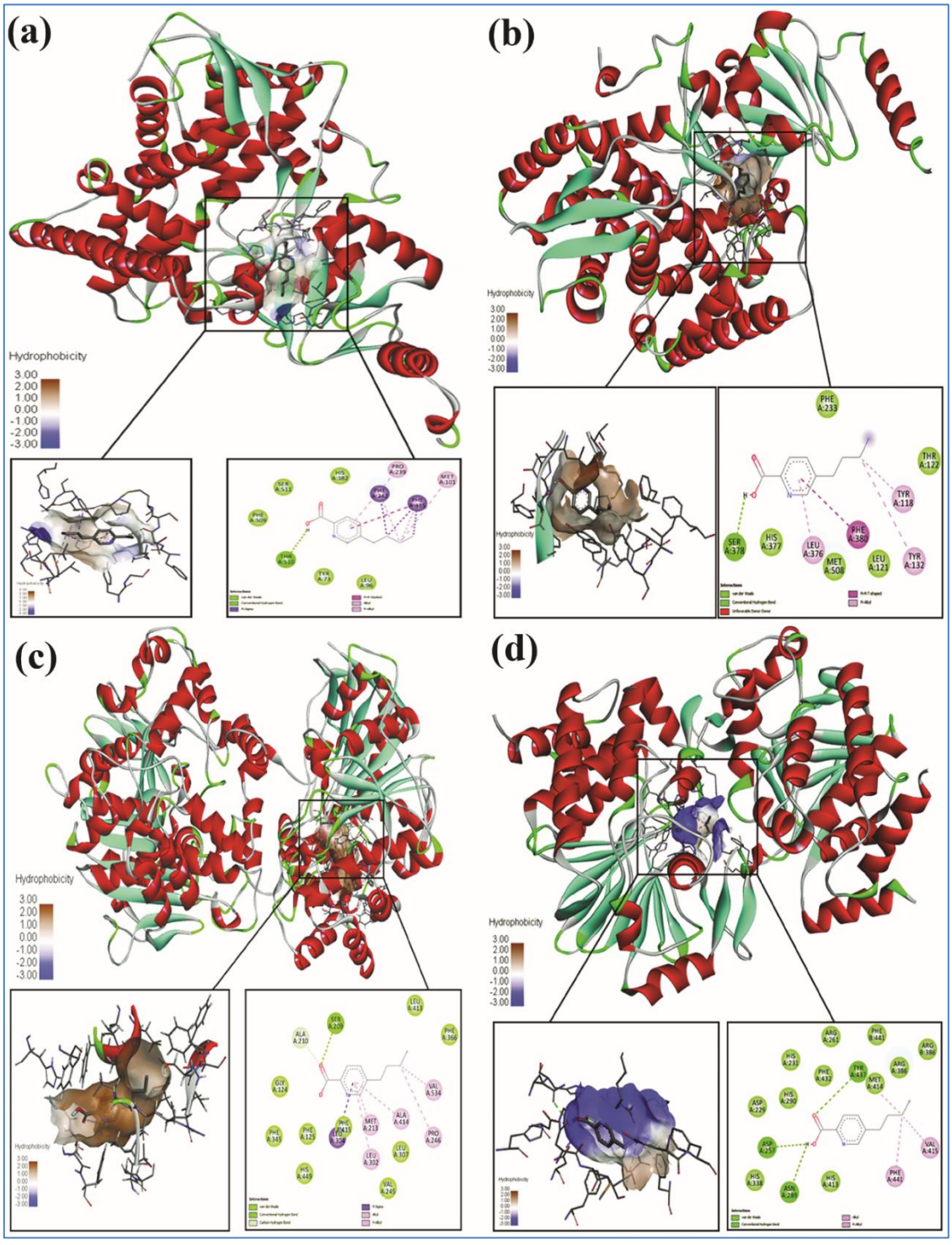


Fig. 4: Molecular docking analysis of protein-ligand (5-butyl-2-pyridine carboxylic acid) interactions against (a) CYP51 from *C. glabrata* (PDB ID 5JLC), (b) CYP51 from *C. albicans* (PDB ID 5V5Z), (c) Cholesterol Esterase of *C. cylindracea* (PDB ID 1LLF), and (d) Yeast-specific serine/threonine protein phosphatase (PPZ1) of *C. albicans* (PDB ID 5JPE).

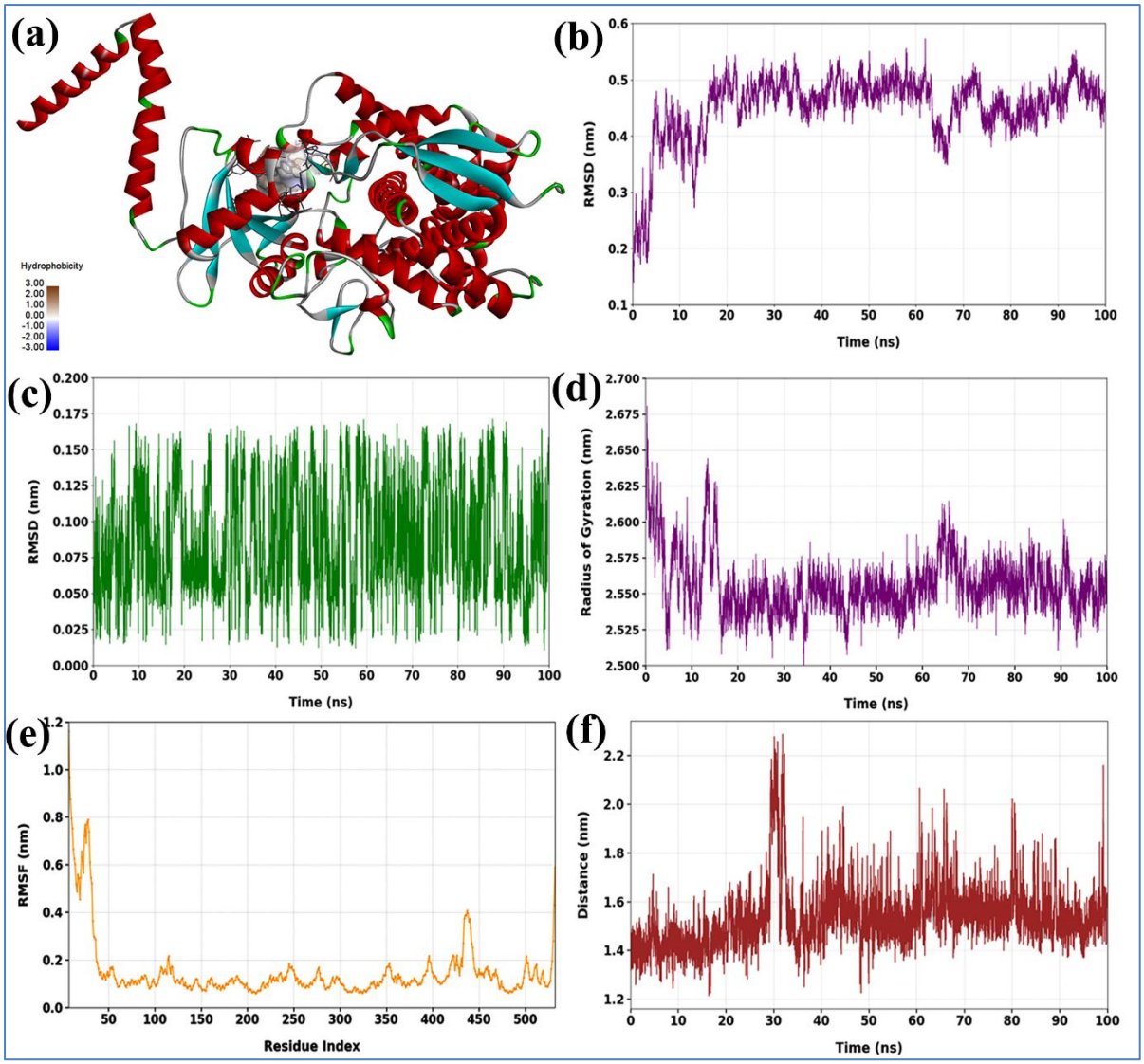


Fig. 5. Molecular dynamics simulation of CYP51 from *C. glabrata* (PDB ID 5JLC) with 5-butyl-2-pyridine carboxylic acid. Here, (a) Model of protein-ligand (5-butyl-2-pyridine carboxylic acid) interactions against CYP51 from *C. glabrata* (PDB ID 5JLC). RMSD profiles over the 100 ns simulation for the protein backbone (b) and the ligand (c) relative to their initial conformations. The protein RMSD reflects overall structural stability, while the ligand RMSD also indicates the stability of the ligand within the binding site. (d) Time evolution of the radius of gyration (Rog) of the protein C_α atoms over the 100 ns simulation, indicating overall compactness and global conformational stability of the protein. (e) Root Mean Square Fluctuation (RMSF) of protein C_α atoms over the 100 ns simulation run, highlighting flexible regions and comparatively rigid core segments along the protein sequence. (f) Time evolution of the protein-ligand distance over the 100 ns molecular dynamics simulation, reflecting the stability and fluctuations of the ligand relative to the protein binding site.

Discussion

The antifungal efficacy of 5-butyl-2-pyridine carboxylic acid observed in this study highlights the therapeutic relevance of low-molecular-weight heteroaromatic fungal metabolites, a class that remains comparatively underexplored against *Candida* spp. The compound exhibited broad-spectrum anti-*Candida* activity, as evidenced by clear growth inhibition zones and low MIC and MFC values against all tested species (Table 1). Notably, *C. tropicalis* demonstrated the highest susceptibility (MIC 0.064 mg/mL), while *C. glabrata* and *C. parapsilosis* required higher fungicidal concentrations. The fungicidal profile of the compound, inferred from MIC–MFC relationships and killing kinetics, suggests irreversible cellular damage rather than growth suppression. Such fungicidal behaviour is clinically advantageous, particularly in invasive candidiasis, where fungistatic agents are often associated with relapse and persistence (Soczó, 2007; Perfect, 2017; Pappas et al., 2018). The MFC values correlated well with time-kill results, suggesting that this compound exerts potent fungicidal activity against a broad range of *Candida* spp. (Soczó, 2007). Interestingly, previous studies with posaconazole reported that, though the compound had relatively low MICs (0.06-0.12 mg/L), no fungicidal effect was observed even at concentrations 16 times the MIC against *C. glabrata* (Soczó, 2007). These species-specific susceptibility patterns observed among *Candida* spp. are consistent with known differences in membrane sterol composition, cell wall architecture, and intrinsic drug tolerance, particularly in *C. glabrata* and *C. parapsilosis* (Arendrup & Patterson, 2017).

Growth and viability assays further substantiated the fungicidal nature of 5-butyl-2-pyridine carboxylic acid (Figures 1 and 2). At 2×MIC, the compound induced rapid loss of viability, with complete killing observed within 3 h in *C. glabrata* and within 9–15 h in other species. Unlike luliconazole, which showed partial regrowth of *C. glabrata*, the test compound 5-butyl-2-pyridine carboxylic acid produced sustained killing without recovery, suggesting reduced adaptive tolerance or resistance development. This persistent antifungal effect is particularly relevant in managing infections caused by *C. glabrata*, a species well known for azole tolerance and treatment failure (Glöckner & Cornely, 2015; Whaley & Rogers, 2016; Hassan et al., 2021). Time-kill kinetics corroborated these observations by demonstrating a ≥3 log CFU/mL reduction within a relatively short exposure period (Figure 2a) (McGinnis and Rinaldi, 1996; Espinel-Ingroff et al., 2002; Hall et al., 2017). The abrupt decline in *C. glabrata* viability within 30 min indicates a rapid cellular target, likely involving membrane-associated damage or disruption of essential metabolism (Figure 2a). This rapid decline in fungal viability following exposure to 5-butyl-2-pyridine carboxylic acid supports a fast-acting cellular target, distinguishing it from several azole antifungals that require prolonged exposure to exert fungistatic effects. Notably, the absence of post-treatment

regrowth, especially in *C. glabrata*, suggests limited adaptive tolerance, an issue frequently reported with azole therapy (Whaley et al., 2017). This sustained killing effect of 5-butyl-2-pyridine carboxylic acid strengthens the compound's potential utility against azole-tolerant or recalcitrant *Candida* infections.

Mechanistic assays indicate that membrane integrity is a key target of the compound. *Candida* spp. possess a rigid β-glucan-chitin cell wall skeleton that provides structural strength and shape (García-Rubio et al., 2020). The LDH leakage assay revealed significant membrane damage in *C. glabrata*, and SEM observations showed that exposure of *C. glabrata* to the compound caused significant rupture and dissolution of the cell wall within 30 minutes, whereas *C. albicans* displayed surface blebbing and pore formation (Figure 2c-2f). These findings strongly suggest that the compound compromises cellular integrity, leading to leakage of intracellular contents and irreversible cell death. The absence of pronounced LDH release in some species despite reduced viability indicates that additional intracellular targets may also be involved (Figure 2b), supporting a multi-target antifungal mechanism rather than exclusive membrane lysis, which is increasingly recognised as beneficial in reducing resistance development (Cheesman et al., 2017). Similar membrane-disruptive effects have been reported for other antifungal secondary metabolites, where loss of membrane homeostasis leads to rapid cell death (Ruan et al., 2021; Mandal et al., 2022).

5-butyl-2-pyridine carboxylic acid effectively inhibited biofilm formation in *C. albicans*, *C. glabrata*, and *C. parapsilosis*, with inhibition rates exceeding 65% at MIC (Figure 3a). The ability of the compound to inhibit biofilm formation and partially destabilise preformed biofilms is particularly noteworthy (Figure 3b), given the central role of biofilms in antifungal resistance and device-associated infections (Sharma, 2019). Although reduced antibiofilm efficacy against *C. tropicalis* was observed, this aligns with prior reports describing the dense extracellular matrix and heightened resilience of *C. tropicalis* biofilms (Madduri et al., 2025). Nonetheless, even moderate biofilm disruption is therapeutically relevant, as it may enhance antifungal penetration and immune clearance (Walla, 2019).

Synergistic antifungal strategies are becoming increasingly important for overcoming resistance in pathogenic fungi. While synergism is commonly reported with antibiotics, it is less frequently documented among antifungal agents (Cheesman, 2017; Matthew, 2019). Combination studies further reinforce the translational potential of 5-butyl-2-pyridine carboxylic acid (Tabl2 2). Synergistic and additive interactions with azole antifungals suggest complementary or sequential targeting of fungal cellular processes. In this context, combination studies have shown that 5-butyl-2-pyridine carboxylic acid significantly enhances the efficacy of imidazole drugs such as luliconazole and clotrimazole, resulting in more potent antifungal activity than monotherapy. Luliconazole and

clotrimazole, both belonging to the imidazole class, act primarily by interfering with ergosterol biosynthesis, thereby compromising fungal membrane integrity (Khanna et al., 2014; Khatter, 2024). Such combinatorial strategies are increasingly advocated to enhance efficacy, reduce drug dosage, and mitigate the evolution of resistance (Gao et al., 2022). Additional evidence of synergy includes the fluconazole-doxycycline combination, which inhibited dual-species biofilms of *C. albicans* and *S. epidermidis* (Gao et al., 2022), as well as hypocrellin-nystatin combinations that enhanced cytotoxicity against *C. albicans* (Song, 2021). Ethosomal formulations of luliconazole with *Azadirachta indica* (neem) extract have also demonstrated synergistic inhibition of *C. parapsilosis* (Dave, 2020). These studies highlight the therapeutic potential of combination therapy and suggest that 5-butyl-2-pyridine carboxylic acid could serve as an effective lead molecule for synergistic antifungal strategies with the imidazole group of drugs.

Molecular docking and enzymatic assays suggest that lanosterol 14α-demethylase (CYP51), a key enzyme in ergosterol biosynthesis, is a primary target of the compound (Figures 4 and 5). Notably, CYP51 is also inhibited by clinically used azoles; however, 5-butyl-2-pyridine carboxylic acid appears to exhibit a stronger and mechanistically distinct inhibitory profile. Comparative analyses of CYP51 inhibition have demonstrated that fluconazole acts as a relatively weak inhibitor, whereas posaconazole shows potent inhibitory activity (Hargrove et al., 2017). The activity pattern observed for 5-butyl-2-pyridine carboxylic acid closely parallels that of stronger azoles, supporting a dual mode of antifungal action involving both membrane disruption and CYP51 inhibition. In addition to CYP51 and its isoform ERG11p, in silico target prediction identified 5-butyl-2-pyridine carboxylic acid as a potential inhibitor of cholesterol esterase from *Candida cylindracea* (PDB ID: 1LLF) and the yeast-specific serine/threonine protein phosphatase PPZ1 of *Candida albicans* (PDB ID: 5JPE), consistent with inhibition profiles reported for benzoflavone derivatives (Singh et al., 2018).

Comprehensive molecular dynamics (MD) analyses, including RMSD, radius of gyration (Rg), RMSF, and intermolecular distance measurements, provide a coherent view of the CYP51–ligand interaction dynamics. Following a brief equilibration phase marked by moderate structural relaxation and compaction, the system attains a stable, long-lived conformation. Throughout the 100 ns simulation, the protein maintains a compact fold, the ligand remains stably accommodated within the active-site pocket, and no major destabilizing events are observed. Notably, the system exhibits dynamic behavior characterized by localized flexibility and transient fluctuations rather than rigid stability, a hallmark of biologically relevant protein–ligand interactions that depend on a balance between structural stability and conformational adaptability. Collectively, these findings demonstrate that the CYP51–5-butyl-2-pyridine carboxylic acid complex remains structurally stable over the simulated timescale,

thereby inhibiting ergosterol biosynthesis in *Candida* sp. This impairment of ergosterol biosynthesis caused cell membrane leakage, as evidenced by the release of lactate dehydrogenase from the organism's cytosol (Fig. 6). Beyond its demonstrated fungicidal activity, 5-butyl-2-pyridine carboxylic acid shows promise as a potential combination therapy partner against multidrug-resistant *Candida* species. Its predicted multi-target inhibitory potential, coupled with favorable toxicity and drug-likeness properties, underscores its therapeutic relevance (Lo et al., 2020). Overall, the results provide compelling evidence that 5-butyl-2-pyridine carboxylic acid represents a promising antifungal drug candidate with a distinct target-specific mechanism of action.

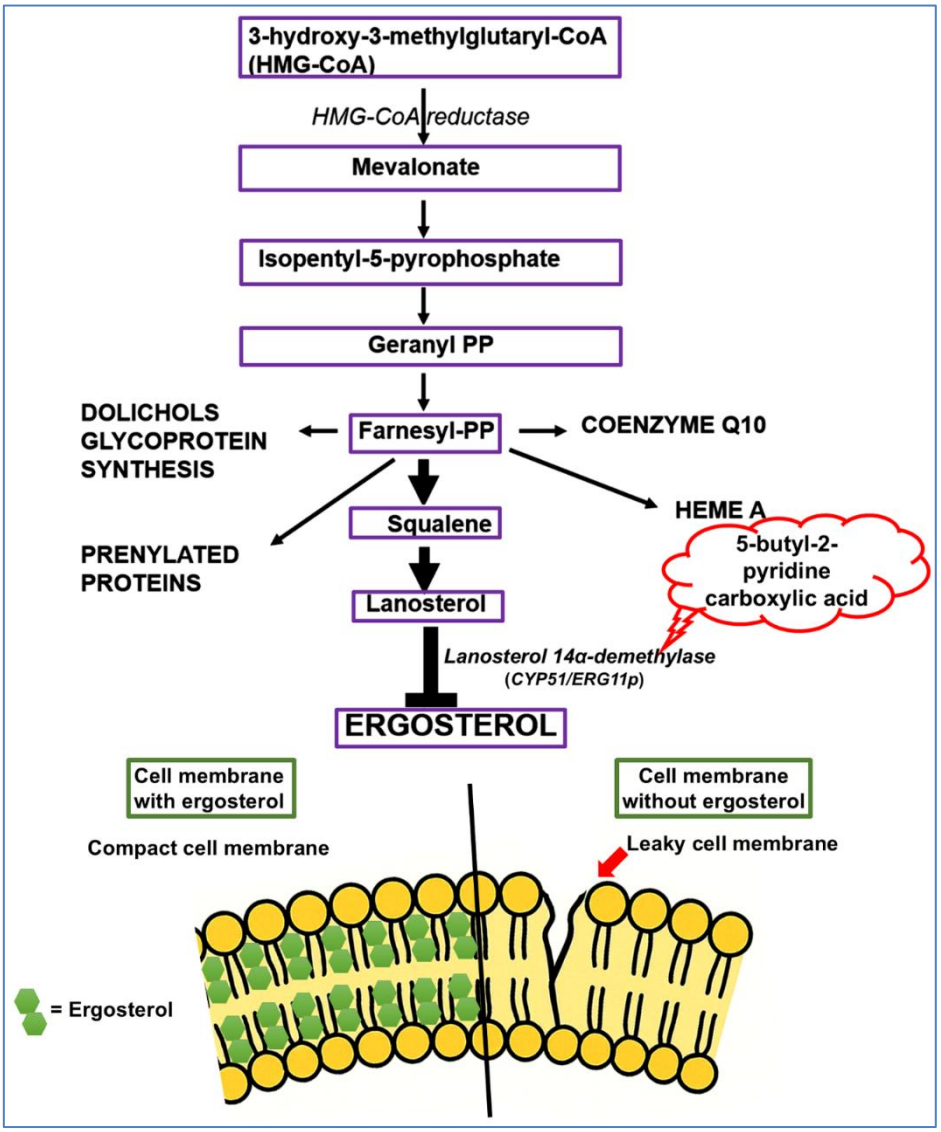


Fig. 6: Proposed mode of action of 5-butyl-2-pyridine carboxylic acid on the cell membrane of *Candida* sp.

Conclusion

The study concludes that 5-butyl-2-pyridine carboxylic acid produced by *Aspergillus fumigatus* nHF-01 exhibits potent anti-*Candida* activity against clinically important species. When many azole drugs fail to cause complete lethality, this novel compound exerts cidal activity by disrupting cellular integrity, as evidenced by membrane damage, pore formation, and cytosolic enzyme leakage, indicating a multi-target mode of action. The compound targets lanosterol 14α-demethylase (CYP51), an enzyme in the key ergosterol biosynthesis pathway, with stable protein–ligand interactions and favourable predicted pharmacokinetic and toxicological profiles. Notably, it also shows synergistic and additive interactions with clinically used imidazole antifungals, such as Clotrimazole and Luliconazole, highlighting its potential in combination therapy. The compound also inhibited biofilm formation and partially destabilised mature biofilms, addressing a significant limitation of current antifungal therapies. Overall, these findings establish 5-butyl-2-pyridine carboxylic acid as a promising anti-*Candida* lead with fungicidal, antibiofilm, and synergistic properties, warranting further in vivo and translational investigation. This is the first report of such a compound from *A. fumigatus* with potent anti-*Candida* activity.

Statements and Declarations

Competing Interests: The authors declare that they have no conflict of interest.

Funding: This research did not receive any specific grant from funding agencies in the public, commercial, or not-for-profit sectors; however, institutional funds and equipment facilities were used for this study.

Data Availability Statement: The data that support the findings of this study are available from the corresponding author upon reasonable request.

Ethical approval: This manuscript has only been submitted to this journal.

Consent to participate: Not applicable

Consent to publish: The Authors consent to publish this work. No other participant was involved.

Acknowledgments

The authors are grateful to the WB DBT-supported BOOST program (2017-2018) (Ref. No. 1089/BT(Estt)/1P-07/2018; dated 24.01.2019) for the equipment grant to the department.

Author contributions:

Conceptualisation: Vivekananda Mandal; **Data curation:** Vivekananda Mandal, and Rajsekhar Adhikary; **Formal analysis:** Vivekananda Mandal, Rajsekhar Adhikary, Narendra Nath Ghosh; **Investigation:** Vivekananda Mandal; **Methodology:** Vivekananda Mandal, Rajsekhar Adhikary; **Project administration:** Vivekananda Mandal; **Resources:** Vivekananda Mandal; **Software:** Rajsekhar Adhikary, Sayan Poddar; **Supervision:** Vivekananda Mandal; **Validation:** Vivekananda Mandal, Rajsekhar Adhikary, Narendra Nath Ghosh; **Visualisation:** Vivekananda Mandal, Rajsekhar Adhikary, Sayan Poddar; **Writing – original draft:** Vivekananda

Mandal, Rajsekhar Adhikary, Narendra Nath Ghosh, Sayan Poddar; **Writing – review and editing:** Vivekananda Mandal

References

Adhikary, R., Maiti, P. K., Ghosh, N., Rajbanshi, B., Roy, M. N., Mandal, S., & Mandal, V. (2025). Lipopeptide iturin C_3 from endophytic *Bacillus* sp. effectively inhibits biofilm formation and prevents the adhesion of topical and food-borne pathogens in vitro and on biomedical devices. Archives of Microbiology, *207*(3), 62. https://doi.org/10.1007/s00203-025-04253-y

Arendrup, M. C. (2013). *Candida* and *Candidaemia*: Susceptibility and epidemiology. *Mycoses, 56*(1), 12–23. https://doi.org/10.1111/myc.12036

Arendrup, M. C., & Patterson, T. F. (2017). Multidrug-resistant Candida: Epidemiology, molecular mechanisms, and treatment. The Journal of Infectious Diseases, 216(suppl_3), S445–S451. https://doi.org/10.1093/infdis/jix131

Bilal, H., Zhang, D., Shafiq, M., Khan, M. N., Chen, C., Khan, S., Wang, Q., Cai, L., Islam, R., Hu, H., & Zeng, Y. (2023). Six-year retrospective analysis of epidemiology, risk factors, and antifungal susceptibilities of candidiasis from a tertiary care hospital in South China. Microbiology Spectrum, 11(4), e0070823. https://doi.org/10.1128/spectrum.00708-23

Blasi, E., Mazzolla, R., Barluzzi, R., Mosci, P., Bartoli, A., Puliti, M., & Bistoni, F. (1993). Intracerebral candidiasis in mice: Immunohistochemical studies and association with microglial cell activation. *Journal of Clinical Investigation, 91*(6), 2777–2784. https://doi.org/10.1172/JCI116518

Cabrera-Guerrero, J. P., García-Salazar, E., Hernandez Silva, G., Chinney Herrera, A., Martínez-Herrera, E., Pinto-Almazán, R., Frías-De-León, M. G., & Castro-Fuentes, C. A. (2025). Candidemia: An Update on Epidemiology, Risk Factors, Diagnosis, Susceptibility, and Treatment. Pathogens, 14(8), 806. https://doi.org/10.3390/pathogens14080806

Cheesman, M. J., Ilanko, A., Blonk, B., & Cock, I. E. (2017). Developing new antimicrobial therapies: Are synergistic combinations of plant extracts/compounds with conventional antibiotics the solution? Pharmacognosy Reviews, 11(22), 57–72. https://doi.org/10.4103/phrev.phrev_21_17

Dave, V., Yadav, R. B., Kushwaha, K., Yadav, S., Sharma, S., & Agrawal, U. (2020). Ethosomal gel of luliconazole and neem extract for treatment of fungal infection: In vitro and in vivo study. Artificial Cells, Nanomedicine, and Biotechnology, 48(1), 270–282. https://doi.org/10.1080/21691401.2019.1709862

Del Palacio, A., Garau, M., & González, F. (2009). Epidemiology and diagnosis of invasive candidiasis: A focus on species distribution. Clinical Microbiology and Infection, *15*(4), 401–407. https://doi.org/10.1111/j.1469-0691.2009.02878.x

Espinel-Ingroff, A., Chaturvedi, V., Fothergill, A., & Rinaldi, M. G. (2002). Optimal testing conditions for determining MICs and minimum fungicidal concentrations of new and established antifungal agents for

uncommon molds: NCCLS collaborative study. Journal of Clinical Microbiology, 40(10), 3776-3781. https://doi.org/10.1128/jcm.40.10.3776-3781.2002

Fatsis-Kavalopoulos, N., Sánchez-Hevia, D. L., & Andersson, D. I. (2024). Beyond the FIC index: the extended information from fractional inhibitory concentrations (FICs). Journal of Antimicrobial Chemotherapy, 79(9), 2394-2396. https://doi.org/10.1093/jac/dkae233

Gao, Y., Zhang, Z., Lun, Z., Gong, L., Xu, A., & Li, X. (2022). Synergistic Effects of Fluconazole Combined with Doxycycline Against Dual-Species Cultures of *Candida albicans* and *Staphylococcus epidermidis* and the Mechanisms of Action. *Microbial drug resistance (Larchmont, N.Y.)*, *28*(5), 525–535. https://doi.org/10.1089/mdr.2021.0301

García-Rubio, R., de Oliveira, H. C., Rivera, J., & Trevijano-Contador, N. (2020). The fungal cell wall: Candida, Cryptococcus, and Aspergillus species. Frontiers in Microbiology, 10, 2993. https://doi.org/10.3389/fmicb.2019.02993

Glöckner, A., & Cornely, O. (2015). *Candida glabrata*–unique features and challenges in the clinical management of invasive infections. Mycoses, 58(8), 445-450. https://doi.org/10.1111/myc.12348

Hall, D., Bonifas, R., Stapert, L., Thwaites, M., Shinabarger, D. L., & Pillar, C. M. (2017). In vitro potency and fungicidal activity of CD101, a novel echinocandin, against recent clinical isolates of *Candida* spp. Diagnostic Microbiology and Infectious Disease, 89(3), 205-211. https://doi.org/10.1016/j.diagmicrobio.2017.07.007

Hargrove, T. Y., Friggeri, L., Wawrzak, Z., Qi, A., Hoekstra, W. J., Schotzinger, R. J., York, J. D., & Lepesheva, G. I. (2017). Structural analyses of *Candida albicans* sterol 14α-demethylase complexed with azole drugs: Insights into antifungal drug resistance. Journal of Biological Chemistry*, 292*(17), 6772–6783. https://doi.org/10.1074/jbc.M116.774802

Hargrove, T. Y., Wawrzak, Z., Liu, J., Nes, W. D., Guengerich, F. P., & Lepesheva, G. I. (2017). Structural analyses of Candida albicans sterol 14α-demethylase complexed with azole drugs: Insights into antifungal drug resistance. Journal of Biological Chemistry, 292(17), 6724–6733. https://doi.org/10.1074/jbc.M117.777334

Hassan, Y., Chew, S.Y., & Than, L.T.L. (2021). *Candida glabrata*: pathogenicity and resistance mechanisms for adaptation and survival. Journal of Fungi, 7(8), 667. https://doi.org/10.3390/jof7080667

Haynes, K. (2001). Virulence in *Candida* species. Trends in Microbiology, 9(12), 591-596. https://doi.org/10.1016/S0966-842X(01)02237-5

Healey, K. R., Jimenez Ortigosa, C., Shor, E., & Perlin, D. S. (2016). Genetic drivers of multidrug resistance in *Candida glabrata*. Frontiers in Microbiology, 7, 1995. https://doi.org/10.3389/fmicb.2016.01995

Khanna, D., Bharti, S. K., & Lall, N. (2014). Antifungal imidazoles: Current perspectives. Current Medicinal Chemistry, 21(26), 3211–3229. https://doi.org/10.2174/0929867321666140514123451

Khatter, N. J. (2024). Mechanistic insights into clotrimazole action on ergosterol biosynthesis and membrane disruption in Candida spp. Mycoses. Advance online publication. https://doi.org/10.1111/myc.13728

Lo, W. H., Lai, Y. H., & Hu, C. K. (2020). Combination antifungal therapy: Prospects and future directions. *Journal of Fungi, 6*(4), 133. https://doi.org/10.3390/jof6040133

Lo, W.-H., Chen, Y.-H., & Hsueh, P.-R. (2020). New perspectives on antifungal combination therapy for invasive fungal infections. Journal of Microbiology, Immunology and Infection, 53(5), 657–666. https://doi.org/10.1016/j.jmii.2019.11.002

Madduri, M., Rudramurthy, S. M., & Roy, U. (2025). Unveiling the in vitro antibiofilm efficacy of antifungal lipopeptides purified from *Bacillus* sp. against mixed-species biofilms of *Candida*. ACS Omega, 10(48), 58671–58687. https://doi.org/10.1021/acsomega.5c06938

Mandal, V., Ghosh, N. N., Mitra, P. K., Mandal, S., & Mandal, V. (2022). Production and characterization of a broad-spectrum antimicrobial 5-butyl-2-pyridine carboxylic acid from Aspergillus fumigatus nHF-01. Scientific Reports, 12(1), 6006. https://doi.org/10.1038/s41598-022-09925-z

Marchetti, O., Moreillon, P., Glauser, M. P., Bille, J., & Sanglard, D. (2000). Potent synergism of the combination of fluconazole and cyclosporine in *Candida albicans*. Antimicrobial Agents And Chemotherapy, 44(9), 2373-2381. https://doi.org/10.1128/aac.44.9.2373-2381.2000

Matthew, T. (2019). Synergistic antifungal therapy: Current developments and future directions. Journal of Fungi, 5(3), 81. https://doi.org/10.3390/jof5030081

McCarty, T. P., & Pappas, P. G. (2016). Invasive candidiasis. Infectious Disease Clinics of North America, 30(1), 103–124. https://doi.org/10.1016/j.idc.2015.10.013

McGinnis, M. R., and M. G. Rinaldi. (1996) Antifungal drugs: mechanisms of action, drug resistance, susceptibility testing, and assays of activity in biologic fluids, p. 176–211. In: V. Lorian (ed.), Antibiotics in Laboratory Medicine. The Williams & Wilkins Co., Baltimore, Md.

Mishra, A. A., & Koh, A. Y. (2021). The microbial and host factors that govern Candida gastrointestinal colonization and dissemination. Current Opinion in Microbiology, 63, 29–35. https://doi.org/10.1016/j.mib.2021.05.012

Ng, K. P., Kuan, C. S., Kaur, H., Na, S. L., Atiya, N., & Velayuthan, R. D. (2015). *Candida* species epidemiology 2000–2013: a laboratory-based report. Tropical Medicine & International Health, 20(11), 1447-1453. https://doi.org/10.1111/tmi.12577

Odds, F. C. (1987). *Candida infections: An overview*. Critical Reviews in Microbiology, 15(1), 1–5. https://doi.org/10.3109/10408418709104435

Oluwole, O. M., Kolawole, O. D., & Olawale, O. S. (2022). *Candida* biofilms: Pathogenesis, clinical implications, and management strategies. Journal of Fungi, *8*(3), 250. https://doi.org/10.3390/jof8030250

Pappas, P. G., Lionakis, M. S., Arendrup, M. C., Ostrosky-Zeichner, L., & Kullberg, B. J. (2018). Invasive candidiasis. Nature Reviews. Disease Primers, 4, 18026. https://doi.org/10.1038/nrdp.2018.26

Perfect, J. R. (2017). The antifungal pipeline: A reality check. Nature Reviews Drug Discovery, 16(9), 603–616. https://doi.org/10.1038/nrd.2017.46

Pfuller, K., Ludwig, R., & Wetzker, R. (2011). Epidemiological aspects of Candida infections. Mycoses, 54(5), 467–474. https://doi.org/10.1111/j.1439-0507.2010.01887.x

Riera, F. O., Caeiro, J. P., Angiolini, S. C., Vigezzi, C., Rodriguez, E., Icely, P. A., & Sotomayor, C. E. (2022). Invasive Candidiasis: Update and Current Challenges in the Management of This Mycosis in South America. Antibiotics, 11(7), 877. https://doi.org/10.3390/antibiotics11070877

Ruan, X., Chen, Z., & Li, Y. (2021). Mechanisms of Candida albicans biofilm development and resistance. Journal of Applied Microbiology, 130(6), 1733–1742. https://doi.org/10.1111/jam.14976

Ruan, X., Zhang, Y., Zhang, T., & Liu, Z. (2021). Antibiofilm activity of novel antifungal compounds against *Candida* biofilms. *Frontiers in Cellular and Infection Microbiology, 11*, 675421. https://doi.org/10.3389/fcimb.2021.675421

Sanglard, D., & Odds, F. C. (2002). Resistance of *Candida* species to antifungal agents: molecular mechanisms and clinical consequences. The Lancet Infectious Diseases, 2(2), 73-85. https://doi.org/10.1016/S1473-3099(02)00181-0

Scully, C., El-Kabir, M., & Samaranayake, L. P. (1994). *Candida* and oral candidosis: A review. Critical Reviews in Oral Biology and Medicine, 5(2), 125–157. https://doi.org/10.1177/10454411940050020101

Sharma, D. (2019). Biofilm resistance mechanisms in pathogenic fungi. Journal of Applied Microbiology, 126(2), 337–350. https://doi.org/10.1111/jam.14121

Silva, S., Negri, M., Henriques, M., Oliveira, R., Williams, D. W., & Azeredo, J. (2012). *Candida glabrata*, *Candida parapsilosis* and *Candida tropicalis*: Biology, epidemiology, pathogenicity and antifungal resistance. FEMS Microbiology Reviews, 36(2), 288–305. https://doi.org/10.1111/j.1574-6976.2011.00278.x

Singh, J. V., Kaur, A., Bhagat, K., Gupta, M. K., Singh, M., Singh, H., & Bedi, P. M. S. (2018). 5,6-Benzoflavones as cholesterol esterase inhibitors: synthesis, biological evaluation, and docking studies. MedChemComm, 9(3), 490–502. https://doi.org/10.1039/c7md00565b

Sobel, J. D. (2007). Vulvovaginal candidosis. The Lancet, 369(9577), 1961–1971. https://doi.org/10.1016/S0140-6736(07)60917-9

Soczó, G., Kardos, G., & Rozgonyi, F. (2007). Correlation of time–kill studies and minimal fungicidal concentrations of posaconazole and other antifungal agents against Candida species. Antimicrobial Agents and Chemotherapy, 51(4), 1514–1517. https://doi.org/10.1128/AAC.01264-06

Soliman, S. (2017). Candida biofilm: Impact on infection and antifungal therapy. *Current Fungal Infection Reports, 11*(2), 56–64. https://doi.org/10.1007/s12281-017-0283-9

Song, S., Liu, Y., Wang, Y., & Zhou, Y. (2021). Synergistic antifungal activity of hypocrellins with nystatin against Candida albicans. Frontiers in Microbiology, 12, 633874. https://doi.org/10.3389/fmicb.2021.633874

Walla, G., & Kullberg, B. J. (2019). Biofilm formation in Candida infections: Pathogenesis, diagnosis and treatment. Current Opinion in Infectious Diseases, 32(6), 610–616. https://doi.org/10.1097/QCO.0000000000000594

Whaley, S. G., & Rogers, P. D. (2016). Azole resistance in *Candida glabrata*. Current Infectious Disease Reports, 18(12), 41. https://doi.org/10.1007/s11908-016-0554-5

Whaley, S. G., Berkow, E. L., Rybak, J. M., Nishimoto, A. T., Barker, K. S., & Rogers, P. D. (2017). Azole Antifungal Resistance in *Candida albicans* and Emerging Non-*albicans Candida* Species. *Frontiers in microbiology*, *7*, 2173. https://doi.org/10.3389/fmicb.2016.02173

Legend to figures:

Fig. 1: Effect of the compound and two standard drugs on the growth and viability of *Candida* strains. The figure indicates the treatment against (**a**) *C. albicans,* (**b**) *C. glabrata,* (**c**) *C. parapsilosis,* and (**d**) *C. tropicalis.* Herein, the blue, red, green, and violet lines indicate the untreated control set, the clotrimazole-treated, the luliconazole-treated, and the 5-butyl-2-pyridine carboxylic acid-treated, respectively, at MIC×2 doses.

Fig. 2: Mode of action of 5-butyl-2-pyridine carboxylic acid. **(a)** Time-kill kinetics; **(b)** Effect of AMC on cellular integrity. Here, in the figure, LDH is shown as bars, and the respective CFU are shown as dotted lines. Here, the bar and line color indicates yellow for *C. albicans,* violet for *C. glabrata,* green for *C. parapsilosis* and black for *C. tropicalis*; and **(c-f)** SEM photomicrographs of *C. albicans* and *C. glabrata* cells treated with 5-butyl-2-pyridine carboxylic acid after 30 min, Here (**c** and **e**) Untreated control cells of *C. albicans* and *C. glabrata* (magnification: ×12000, ×3000, respectively); (**d**) Treated *C. albicans* cells after 3 h incubation (magnification: ×8500); (**f**) Treated *C. glabrata* cells after 3 h incubation (magnification: ×1900). The significant morphological changes have been marked with red arrows.

Fig. 3: Effect of 5-butyl-2-pyridine carboxylic acid on **(a)** *Candida* biofilm formation inhibition and **(b)** destabilisation of performed biofilm. Here, the bar indicates AMC (5-butyl-2-pyridine carboxylic acid) treatment, and the dotted line indicates Usnic acid (UA) treatment. Here, the bar indicates AMC treatment, and the dotted line indicates Usnic acid treatment.

Fig. 4: Molecular docking analysis of protein-ligand (5-butyl-2-pyridine carboxylic acid) interactions against (a) CYP51 from *C. glabrata* (PDB ID 5JLC) (b) CYP51 from *C. albicans* (PDB ID 5V5Z) (c) Cholesterol Esterase

of *C. cylindracea* (PDB ID 1LLF), and (d) Yeast-specific serine/threonine protein phosphatase (PPZ1) of *C. albicans* (PDB ID 5JPE).

Fig. 5. Molecular dynamic simulation of CYP51 from *C. glabrata* (PDB ID 5JLC) with 5-butyl-2-pyridine carboxylic acid. Here, (a) Model of protein-ligand (5-butyl-2-pyridine carboxylic acid) interactions against CYP51 from *C. glabrata* (PDB ID 5JLC). RMSD profiles over the 100 ns simulation for the protein backbone (b) and the ligand (c) relative to their initial conformations. The protein RMSD reflects overall structural stability, while the ligand RMSD also indicates the stability of the ligand within the binding site. (d) Time evolution of the radius of gyration (Rog) of the protein C_α atoms over the 100 ns simulation, indicating overall compactness and global conformational stability of the protein. (e) Root Mean Square Fluctuation (RMSF) of protein C_α atoms over the 100 ns simulation run, highlighting flexible regions and comparatively rigid core segments along the protein sequence. (f) Time evolution of the protein-ligand distance over the 100 ns molecular dynamics simulation, reflecting the stability and fluctuations of the ligand relative to the protein binding site.

Fig. 6: Proposed mode of action of 5-butyl-2-pyridine carboxylic acid on the cell membrane of *Candida* sp.

Supplementary Files

This is a list of supplementary files associated with this preprint. Click to download.

- MSSupplementary04.08.2026.docx